EARTH SURFACE PROCESSES AND LANDFORMS
Earth Surf. Process. Landforms **41**, 855–864 (2016)

Published online 19 February 2016 in Wiley Online Library
(wileyonlinelibrary.com) DOI: 10.1002/esp.3905

Reconstructing and understanding the impacts of storms and surges, southern North Sea

Sue M. Brooks,[1]* Tom Spencer,[2] Anna McIvor[2] and Iris Möller[2]
[1] Department of Geography, Environment and Development Studies, Birkbeck, University of London, London, UK
[2] Cambridge Coastal Research Unit, Department of Geography, University of Cambridge, Cambridge, UK

Received 6 March 2015; Revised 24 November 2015; Accepted 11 January 2016

*Correspondence to:Sue M. Brooks, Department of Geography, Environment and Development Studies, Birkbeck, University of London, Malet Street, London WC1E 7HX, UK. E-mail: s.brooks@bbk.ac.uk

ESPL
Earth Surface Processes and Landforms

ABSTRACT: Coastal barriers are ubiquitous globally and provide a vital protective role to valuable landforms, habitats and communities located to landward. They are, however, vulnerable to extreme water levels and storm wave impacts. A detailed record of sub-annual to annual; decadal; and centennial rates of shoreline retreat in frontages characterized by both high (> 3 m) and low (< 1 m) dunes is established for a barrier island on the UK east coast. For four storms (2006–2013) we match still water levels and peak significant wave heights against shoreline change at high levels of spatial densification. The results suggest that, at least in the short-term, shoreline retreat, of typically 5–8 m, is primarily driven by individual events, separated by varying periods of barrier stasis. Over decadal timescales, significant inter-decadal changes can be seen in both barrier onshore retreat rates and in barrier extension rates alongshore. Whilst the alongshore variability in barrier migration seen in the short-term remains at the decadal scale, shoreline change at the centennial stage shows little alongshore variability between a region of barrier retreat (at 1.15 m a^{-1}) and one of barrier extension. A data-mining approach, synchronizing all the variables that drive shoreline change (still water level, timing of high spring tides and peak significant wave heights), is an essential requirement for validating models that predict future shoreline responses under changing sea level and storminess. © 2016 The Authors. Earth Surface Processes and Landforms published by John Wiley & Sons Ltd.

KEYWORDS: coastal storms; barrier island dynamics; storm waves; surge residuals; shoreline retreat; DSAS

Introduction

Barrier islands are long, thin, low-lying sand-gravel structures, typically oriented subparallel to a mainland coast and separated from it, to varying degrees, by a coastal lagoon. Accounting for 6 to 15% of the world's total shoreline length (Otvos, 2012), they protect biodiverse and ecologically valuable backbarrier wetlands as well as adjacent mainland coasts from direct storm impacts and erosion. Moreover, barriers themselves support growing residential communities [between 1990 and 2000 the US barrier island population reached 1.4 million, a decadal increase of 14% (Zhang and Leatherman, 2011)] and economically important tourist industries (Fitzgerald *et al.*, 2008). These contexts, therefore, raise significant societal issues as to how barrier systems will respond to near-future global environmental change. Whilst many barrier systems have maintained themselves through landward migration by barrier 'roll-over' over the course of the Holocene transgression (e.g. McBride *et al.*, 2013), there is also evidence in the recent geological record for barrier in-place drowning and subsequent sudden shifts in shoreline position (e.g. Sanders and Kumar, 1975; Mellett *et al.*, 2012). Differing modes of barrier dynamics raise questions about (i) the interactions between rates of sea level rise, natural and anthropogenically-modified sediment supply, and regional bathymetric and topographic settings for barrier stability and (ii) future barrier maintenance, fragmentation and loss in the face of accelerating rates of sea-level rise (Church *et al.*, 2013). A related issue, of immediate concern to lives and livelihoods on barrier islands, is the potential impact of near-future changes, still highly uncertain [Intergovernmental Panel on Climate Change (IPCC), 2013], in the magnitude and frequency of tropical and/or extratropical storms on barrier futures. Reconciling these concerns suggests a need for a more thorough synthesis of barrier dynamics, one which integrates long-term trends with short-term events.

At the process level, sediment transport to the landward side of barrier islands by overwash or through storm-induced breaches is the major driver in roll-over dynamics (Donnelly *et al.*, 2006) and landward overwash flux is a key parameter in many coastal evolution models (e.g. Cowell *et al.*, 1995: Jiménez and Sánchez-Arcilla, 2004). However, it is clear that overwash is not a simple process in either space or time. Sallenger's (2000) storm-impact scaling model defines four storm-impact regimes based on the relative relationship between the elevation of a morphological feature (i.e. sand dune or upper beach ridge) and that of storm-induced water levels (astronomical tide + storm surge + wave runup). The model predicts non-linear morphological change as the water levels associated with larger and larger storms shift runup and wave attack higher up the profile until, in the most extreme impact category (inundation) 'massive net onshore transport occurs with landward migration of sand bodies on the order of 1 km' (Sallenger, 2000, p. 894). More recent studies, however, do not wholly support the argument that morphologic response increases monotonically with impact regime, with variable landscape change at the low impact stages of the Sallenger model and even flow and sediment transport reversal, from the backbarrier seawards, with barrier inundation (e.g. Long *et al.*, 2014).

There is, therefore, a critical need to determine the scales of variability in coastal change on barriers, the magnitude of change at these scales, and the processes responsible for the observed variability (Stockdon *et al.*, 2007). These questions are being addressed through numerical modelling (e.g. Masetti *et al.*, 2008; Moore *et al.*, 2010; Lorenzo-Trueba and Ashton, 2014) and other approaches (e.g. Bayesian Networks: Plant and Stockdon, 2012). They have recently been explored in micro-tidal settings impacted by episodic hurricane and extra-tropical storm landfalls (e.g. North Carolina: Lazarus *et al.*, 2012; Mississippi delta plain: Sherwood *et al.*, 2014). Here, we consider these issues through a data-driven approach for a macro-tidal barrier island setting in the southern North Sea, a region where the interaction of storm surge incidence, twenty-first century sea level rise and changing coastal vulnerability is of considerable concern (Weisse *et al.*, 2014). Since 1992, the UK Environment Agency has been collecting annual vertical aerial photography of the east coast of England and monitoring cross-shore profiles at six monthly intervals. We analyse this information alongside available tidal, surge water level and wave datasets. At longer timescales, we supplement these datasets with archival map evidence and records of historic storm surges; at the event scale, we utilize recent developments in ground survey techniques which allow rapid, accurate measurements of storm impacts. Specifically, we address these issues by the determination of:

1. shoreline change rate (calculated at high densification (10 m interval) over a 5 km barrier frontage) based on three different shoreline pairs (2006 and 2007; 2007 and 2008; 2013 and 2014), six-monthly change at a series of 1 km-spaced shore profiles (2006–2014) and high resolution field surveys post-December 2013 storm, assessing short-term barrier morphological response to storm surge impacts;
2. shoreline change rates representing change at the approximately decadal scale based on three shorelines (1992, 2000, 2008) spanning, eight, eight, and 16 years, respectively;
3. shoreline change rates based on the 1891 and 2013 shorelines representing summary change at the centennial scale.

Location

The barrier island of Scolt Head Island, North Norfolk coast, UK is a National Nature Reserve that has not been subjected to interventionist management and where a long tradition of geomorphological and ecological monitoring extends back to the 1920s (Steers, 1960). The 45 km long, north-facing coastline between Old Hunstanton and Kelling Hard (Figure 1A) experiences a macro-tidal, semi-diurnal tidal regime with a mean spring tidal range of 6.4 m at Hunstanton, declining to 4.7 m at Cromer, 15 km east of the study area. Four inshore wave stations between Scolt Head Island and Horsey recorded annual mean significant wave heights of 0.49 to 0.73 m, September 2006–September 2009 (Environment Agency, 2014). Thus in the Hayes (1979) classification scheme, Scolt Head Island is a 'tide-dominated' barrier island. The combination of high tidal range and low background wave activity with low offshore slopes explains the presence of extensive intertidal environments, developing after 7 ka BP over older basal peats on glaciated surfaces (Andrews *et al.*, 2000). These comprise subtidal mudflats, intertidal sandflats, sand and gravel barriers with ebb tide deltas, tidal channels and barrier-protected salt marshes and mudflats. Extensive reclaimed salt marsh, behind earthen embankments, characterizes much of the landward margin of the intertidal zone (Figure 1B). The coastal topography is dominated by the Weybourne-Cley-Blakeney Point spit complex to the east and the barrier island of Scolt Head Island to the west (Figure 1C). The history of the barrier is one of westward extension, with pauses in this extension being represented by well-developed dune complexes reaching 15–20 m ODN (ODN, Ordnance Datum Newlyn where 0.0 m approximates to mean sea level) and the presence of irregularly-spaced, recurved and landward-trending 'laterals' (Steers, 1960). The sequence of laterals encloses back-barrier salt marshes of progressively decreasing age from east to west (French, 1993). As well as areas of high (> 3 m) dunes, the seaward margin of the barrier is characterized by stretches of low (< 1 m) dunes; unvegetated and partially vegetated, older, inactive washover fans; and, at its western extremity, mobile spits and bars of sands and gravel. In this paper we focus attention largely on the dynamics of the high and low dune sections.

The shallow, semi-enclosed southern North Sea is affected both by external surges, which enter the North Sea from the North Atlantic and propagate southwards as a Kelvin wave with the tide (taking nine hours to travel from Dunbar, Scotland to the outer Thames estuary) and internal surges which are generated by water level set-up from wind stress within the North Sea itself (Pugh and Woodworth, 2014). They are particularly damaging when they coincide with high spring tides and gale-force onshore winds that can generate large peak significant wave heights, resulting in coastal erosion, sea defence breaching and extensive sea flooding on low-lying coasts. Lamb and Frydendahl (1991 chronicle 26 major sea flood events along the North Sea coastline between 120 BC and AD 1978. In modern times, the benchmark event is often seen as the catastrophic storm surge of 31 January–1 February 1953, arguably, in terms of loss of life (> 2000 deaths), the most devastating natural disaster to affect northwest Europe during the last 100 years (Gerritsen, 2005).

Methods

Wave and water level datasets

Between September 2006 and September 2014, there were four major storms/storm surges on the UK east coast. These occurred on 31 October–2 November 2006; 17–21 March 2007; 7–8 November 2007 (Environment Agency, 2009, 2014); 5–6 December 2013 (Spencer *et al.*, 2014). For each storm surge, the time series record of still water level at seven UK east coast tide gauges (see Figure 1A for locations), as well as the surge residual (difference between actual and predicted water level) were obtained from the British Oceanographic Data Centre (BODC) (https://www.bodc.ac.uk/data/online_delivery/ntslf/). All water level data, reported at 15 minute intervals, were converted from local Chart Datum to ODN. The nearest tide gauge to the field site is located at Cromer (52°56′3.70N 001°18′5.90E), 15 km to the east, but unfortunately there is a gap in the data for the 2007 event and little still water level data for the 2013 event, due to wave action beneath Cromer pier severely disrupting the gauge stilling well. Water level records, where data are available, are reported in Supporting Information (Figures S1A–S1D).

Co-varying significant wave height and wave direction data are available for the November 2006, March 2007 and

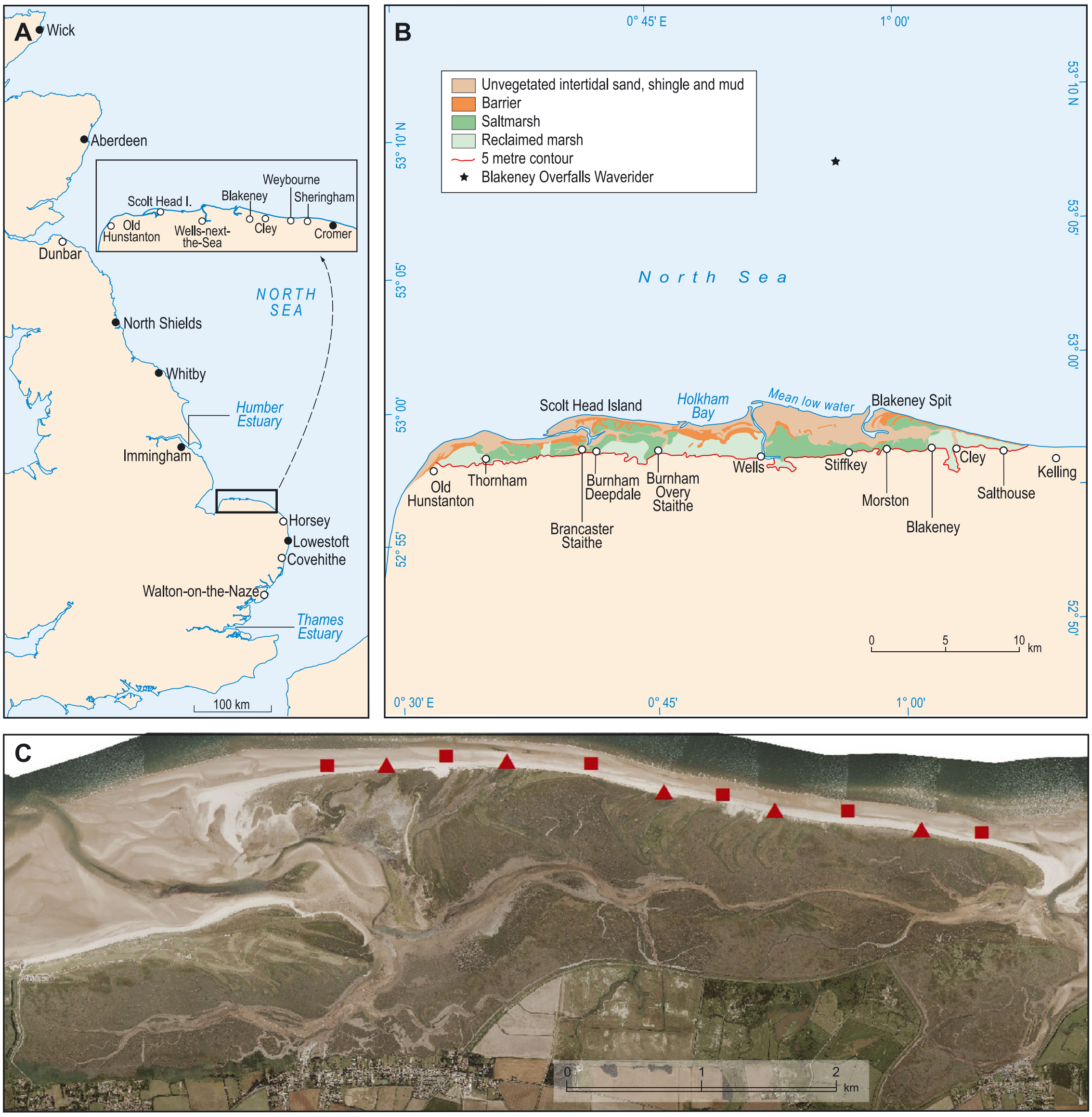

Figure 1. Location and environmental setting of the North Norfolk Coast. (A) UK east coast and North Norfolk coast (inset). Solid circles are tide gauge locations. (B) Landforms and habitats, Old Hunstanton to Kelling, North Norfolk Coast. (C) Scolt Head Island back barrier marsh aerial photograph from August 2014 with symbols showing Environment Agency cross-shore profile locations. Squares show profile locations with data for 2006 to 2007 as well as 2013 to 2014 and triangles show locations with data for just 2013–2014. © Environment Agency copyright and/or database right 2015. All rights reserved. This figure is available in colour online at wileyonlinelibrary.com/journal/espl

November 2007 events at the Scolt Head Island (53°00′.03N 000°41′.06E) inshore (9 m water depth) Acoustic Wave and Current (AWAC) recording station (Figure 1B). This station had been decommissioned by the time of the December 2013 storm. It has been possible, however, to reconstruct a 2013 wave record at Scolt by cross-correlation with the Blakeney Overfalls Wave rider Buoy (53°03′.20N 001°06′.42E; 10 km offshore, 18 m water depth) record which also reports wave characteristics for the two 2007 events. Data were downloaded from the Centre for Environment, Fisheries and Aquatic Systems (CEFAS) website (http://www.cefas.defra.gov.uk/our-science/observing-and-modelling/monitoring-programmes/wavenet.aspx). Whilst the inshore AWAC station recorded data at hourly intervals, the Blakeney Overfalls data are collected at 30 minute intervals.

Morphological datasets and analytical methods

Short-term, event-based shoreline change (2006–2014)

UK Environment Agency cross-shore profile data have been collected in the field every six months ('winter' and 'summer') since 1992, using a differential global positioning system (DGPS) [horizontal and vertical precision of ±20 and ±30 mm, respectively (Lee, 2008)]. These data were used to assess shoreline change at point locations along the barrier (Figure 1C). Initially the profile locations were at 1 km spacing, giving a total of five locations on Scolt Head Island. From summer 2011, additional locations were added to the monitoring programme. However some of the additional cross-shore transects cross washover fans where it is difficult to determine the line of the barrier margin. As a result, they were excluded from the analysis, leaving a total of eight cross-shore locations. By plotting changes in the barrier margin identified on the cross-shore profiles for the most recent part of the record (since summer 2006 – chosen because that date marks the start of the availability of detailed storm data as discussed earlier), periods of significant landward migration, as well as stasis, in shoreline position could be identified.

The ArcMap extension Digital Shoreline Analysis System [DSAS version 4.0 (Thieler *et al.*, 2009)] methodology was then used to quantify in greater spatial detail the changing shoreline position for those years between 2006 and 2014 when significant (> 1 m) shoreline translation had been identified in the cross-shore profiles. Barrier margins were identified on georeferenced annual 'summer' vertical aerial photography and digitized within ArcMap (version 10.1). Georeferencing and digitizing errors are discussed in detail in Brooks and Spencer (2010; they suggest typical accuracy lies within 5% of total shoreline retreat). Shore-normal transects were cast at 10 m alongshore spacing and, using DSAS, the End Point Rate (i.e. rate of shoreline position change, in m a^{-1}) was found for the intersection of each shoreline with each transect. A total of 455 alongshore transects was cast along the barrier, covering almost the 5 km length of shoreline. It was also possible to cross compare shoreline change evident in the cross shore profile with the end point rate (EPR) for the equivalent alongshore transect found using the DSAS methodology.

For the fourth storm (5 December 2013), cross-shore profile (3 September 2013–13 March 2014), summer 2013 and summer 2014 vertical aerial photography datasets DSAS analyses were supplemented with additional field data collected using a Real Time Kinematic (RTK) system (Leica Viva GS08 Global Navigation Satellite System; data screening to ensure three dimensional coordinate quality < 50 mm and typically < 20 mm) between 6 December 2013 and 3 March 2014.

Meso-term shoreline change (1992–2000, 2000–2008)

Late summer vertical aerial photography from 1992, 2000 and 2008, obtained from the UK Environment Agency, was used to assess shoreline change for the periods 1992–2000, 2000–2008 and 1992–2008 (1992 also represents the first year of such data collection by the Agency). These periods were chosen as analysis elsewhere on the UK East Coast, including the Weybourne cliffs at the eastern end of the study area, has shown that these first two periods reflect clearly delineated periods of enhanced and reduced storminess, respectively (Brooks and Spencer, 2013). Shoreline retreat was quantified using an identical methodology to that used for the short-term analysis described earlier.

Long-term shoreline change (1891–2013)

To assess long-term shoreline change we digitized shorelines using (i) the 1891 historic Ordnance Survey map at a scale of 1:10 560 and (ii) the 2013 vertical aerial photograph obtained from the UK Environment Agency. Shorelines were approximated using the mapped mean high water mark of ordinary tides on the 1891 map. On the 2013 aerial photography, the main barrier edge could be defined clearly where the dunes were eroding, but where washover fans were present the edge was obscured so these shoreline sections (totalling a distance of 450 m) were excluded from further analysis. At the actively extending western end of the island, the change from vegetated marsh to mudflat was chosen to represent shoreline position. Again a total of 455 transects was included in the analysis, covering a total alongshore distance of almost 5 km.

Results

Hydrodynamic conditions associated with selected storms, 2006–2013

Still water levels at Immingham and Cromer, the surge residual at Cromer and wave conditions associated with the four storm surges studied in detail are shown in Table I and Figure 2.

Table II sets these storms in the context of the historical record of storm impacts on the North Norfolk coast, 1883–2014. The four storms can be evaluated against the estimated return periods, based on still water levels only, from the three tide gauges at Immingham, Cromer and Lowestoft. Three of these storms were relatively modest according to this criterion, whilst it is clear that the 5–6 December 2013 event was a superstorm [although Haigh *et al.* (2015) believe that the 1953 storm was of comparable magnitude].

The highest still water level reached in the November 2006 event at Cromer was 2.74 m ODN, with a maximum surge residual of 1.65 m. Maximum recorded significant wave heights (H_s) at Scolt Head Island were 2.2 m, coinciding with high tides and surge residuals greater than 1.0 m. Waves remained at these levels through the long duration of the surge (18 hours 45 minutes) and there was then a steady fall in wave heights to around 0.5 m by 1800 on 3 November 2006. For the March 2007 storm, a different pattern is apparent. Surge residuals reached 1.38 m at Cromer but were over 1 m for just 2.5 hours. During this short-lived period, peak significant wave heights were just 1.7 m at Scolt. The maximum surge residual occurred at 14:45 on 18 March while the maximum still water level was reached at 18:00 on the same day when the surge residual had fallen to 0.94 m. Thus although still water levels were high (2.83 m), wave action was limited during the surge itself. The phase of high spring tides continued for the next two days, coinciding with a series of low pressure troughs bringing westerly to northerly winds sustained at Beaufort Force 5–8 (8–21 m s^{-1}). Windspeeds did not drop until late on 20 March 2007. Onshore waves reached significant wave heights of 2.8 m, and a peak wave height (H_{max}) of 5.1 m, at Scolt and were maintained at these levels over two successive high tides on 20 March. The maximum still water level recorded during this period at Cromer was 3.35 m at 18:00 on 18 March, but high water levels occurred over successive high tides when the waves were at their highest. In November 2007 surge residuals > 1 m occurred for eight hours and 45 minutes, developing on a falling tide and coincident with low tide. Hence the maximum still water level attained during this storm at Cromer was 2.70 m. Peak

Table I. Summary of hydrodynamic conditions associated with 4 storms occurring between summer 2006 and summer 2014

	31 October–3 November 2006	17–20 March 2007	7–10 November 2007	4–7 December 2013
Maximum still water level (mOD) Cromer	2.74	3.35	2.70	—
Maximum still water level (mOD) Immingham	3.16	4.21	3.99	5.22
Maximum surge residual (m) Cromer	1.65	1.38	1.86	—
Maximum surge residual (m) Immingham	1.68	0.91	1.67	1.97
Surge residual > 1 m (hours)	18.75	2.50	8.75	14.00
Maximum wave height (m) Scolt	2.20	2.80	2.70	—
Maximum wave height (m) Blakeney	—	3.90	3.50	3.80
Direction of maximum wave (°N) Scolt	6	8	0	—
Direction of maximum wave (°N) Blakeney	—	0	4	338

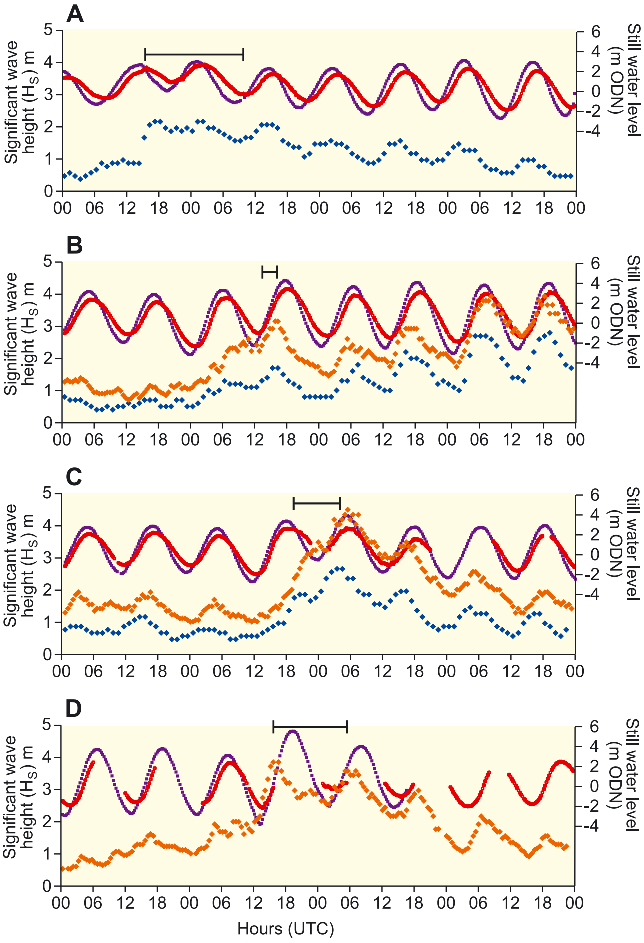

Figure 2. Still water levels (in m ODN) recorded in the tide gauges at Immingham and Cromer and significant wave height (H_s) recorded in the AWAC wave stations at Scolt Head Island (diamonds) and Blakeney (triangles) for the storms of: (A) 31 October–3 November 2006; (B) 17–20 March 2007; (C) 7–11 November 2007; (D) 4–7 December 2013. Also shown are periods when the surge residual at Cromer exceeded 1 m. Tidal data supplied by the British Oceanographic Data Centre as part of the function of the National Tidal and Sea Level Facility, hosted by the Proudman Oceanographic Laboratory and funded by the Environment Agency and Natural Environment Research Council. Wave data courtesy of CeFAS wavenet data archive. This figure is available in colour online at wileyonlinelibrary.com/journal/espl

significant wave heights during the surge were 2.7 m, with these waves also coinciding with low water levels. Following the passage of the surge, recorded wave heights also reached 2.7 m at time of the next high tide. Wave heights then fell away rapidly, being reduced to 1.0 m by 10 November 2007. For the December 2013 storm there is no tide data for Cromer for the peak of the storm. However, it is possible to assess the magnitude of this surge component in comparison to the other three events from still water levels recorded at Immingham. Here the storm surge produced the highest water level on record (1953–2012; Spencer *et al.*, 2014). The surge residual, at 1.97 m, was also the highest recorded for the four storms analysed here and, although it preceded the still water level peak by almost two hours it was maintained at > 1 m to encompass the water level peak. Although the Cromer tide gauge malfunctioned, the surge residual went above 1 m at 15:15 on 5 December and we assume remained above 1 m until 05:15 on 6 December by which time the tide gauge was recording again. Thus the surge residual was > 1 m for 14 hours at Cromer. The peak wave heights recorded at Blakeney Overfalls were 3.8 m, which most probably equates to wave heights of 2.7 m at Scolt (Figure 3). However, wave heights > 3 m were only maintained here for a four hour period (Spencer *et al.*, 2014).

Shoreline dynamics

Short-term (2006–2014)

EPRs from an alongshore DSAS analysis (error term: < 50 cm per 10 m of retreat) are shown for 2006–2007 (Figure 4A), 2007–2008 (Figure 4B) and 2013–2014 (Figure 4C). The retreat between summer 2006 and summer 2007 averaged 0.69 m over the 5 km barrier length. However, large sections of the frontage (55% of the total length) experienced zero landward translation while in places retreat rates reached 5 m. The western end of the island (between 0 and 3 km alongshore), where the retreat was greatest, saw an average retreat of 1.13 ± 0.06 m. The equivalent annual average retreat rate from summer 2007 to summer 2008 was 1.57 ± 0.08 m while between summer 2013 and summer 2014 the mean alongshore retreat was 4.56 ± 0.23 m, with some sections of the shoreline retreating by over 12.00 ± 0.60 m. By comparison, in the period of barrier stasis (2008–2013) it was impossible to conduct a DSAS analysis because the shorelines were so close together once they had been digitized from the aerial photographs that they could not be distinguished from one another without the aerial imagery pixelating, thus blurring the precise location of the shoreline.

Figure 5 shows the change in position of the barrier crest based on cross-shore profile data collected at six-monthly intervals between 6 September 2006 and 8 September 2014. It is clear that significant (> 1 m) barrier retreat characterized the periods 22 January–11 September 2007, 11 September 2007–5 January 2008 and 3 September 2013–13 March 2014.

Finally, we further refine the storm response during the latest period of activity using the RTK field data collected between December 2013 and February 2014. The shoreline position on the 2013 aerial photograph (15 July 2013) compared with the RTK field data produced a mean inland retreat (Net Shoreline Movement) of 8.14 ± 0.39 m along the barrier, while the DSAS analysis based upon the RTK data and the 2014 aerial photograph (31 October 2014) produced a mean seaward movement of the barrier of 0.11 ± 0.01 m, suggesting a slight shoreline recovery in this later period, most probably from the re-establishment of pioneer dunes in front of the eroded dune faces. The average EPR between shorelines in 2013 and 2014 was 4.56 ± 0.23 m a^{-1}.

Meso-term shoreline change (1992–2000, 2000–2008)

Over the meso-term, the retreat rate between 1992 and 2008 was 0.76 m a^{-1}. However, this average rate masks major differences in retreat rate within this period. A mean island retreat rate of 1.22 m a^{-1} was experienced between 1992 and 2000, being over three times that of the period 2000–2008 (0.34 m a^{-1}) (Figure 6A). At the same time, the western end of the island advanced westwards by 35 m between 1992 and 2000, compared with 80 m between 2000 and 2008.

Long-term shoreline change (1891–2013)

From Figure 6B we see that the long-term (1891–2013) average rate of landward retreat along the whole barrier was 1.15 m a^{-1}. It is clear too that the western end of the island, from 1.08 km along the barrier from the westward end has been extending alongshore at an average rate of 2.53 m a^{-1}, with high maximum rates of almost 4 m a^{-1} at the most western extremity, seen in the first 12 cross-shore transects (120 m). Thus the crossover from predominantly alongshore extension to predominantly landward retreat lies at 1.08 km east of the current westernmost end of the island. Thus, in general terms, the island has elongated and moved onshore since 1891. In 1891 the island was 4.35 km long while in 2013 this had extended

Table II. Major storms on the North Norfolk coast, 1883–2013 with (where known) location-specific maximum water levels, still water level return period estimates from regional tide gauges and records of impacts and infrastructural damage

Date	Maximum water level (locations in parentheses; key below table)	Return Period (a1)	Return Period (a2)	Return Period (a3)	Return Period (b1)	Reported impacts and infrastructural damage
11 March 1883	5.49? (5) benchmark not clear					Major flooding at Wells, including quay, Freeman Street. Tramways and earthworks damaged
28 November 1897	4.96 (8); 4.49? (5)					Major coastal flood event; properties flooded at Cley
26 August 1912	4.66 (6)					possibly riverine flash flood rather than storm surge but reported for Cromer on 25 August
12 February 1938	not available					Main coast road flooded at Salthouse. Scolt Head Island suffered erosion, some dunes shortened
8 January 1949	not available					
1 March 1949	not available					Flooding at Brancaster Staithe and Salthouse
31 January 1953	5..49 (1); 5.15 (5; mean level); 5.13 (5; mean level); 4.57 (6; mean level); 6.07 (8; mean level)	21				Regional disaster. Extensive breaching of sea defences and widespread coastal flooding
20 March 1961	not available					
16 February 1962	not available					
29 September 1969	4.43 (3); 4.27 (5)	43		39		
2 January 1976	4.35 (3); 4.46 (5); 4.55 tidegauge	21		33		Flooding at Cley, Salthouse
11 January 1978	4.62 (3); 5.51 (4); 4.91 (5); 5.55 (6); 5.26 (7); 4.90 (8); 5.14 (9)	27		7		Flooding at Holme, Wells, Cley and Salthouse. Major sea defence breach, Wells Harbour Channel
12 December 1990	4.55 (3); 4.67 (4)					Properties flooded along North Norfolk coast
20 February 1993	4.45? (2); 4.41 (5)		9	27		Flooding at Wells and Cley. Overtopping of gravel barrier at Cley and flooding of freshwater marshes
1 January 1995	4.55 (3); 4.54 (4); 4.45 (6); 4.66 (8)		6	7		
19 February 1996	not available					Overtopping of gravel barrier at Cley and flooding of freshwater marshes for 14 days
14 December 2003	not available					Overtopping of gravel barrier at Cley and freshwater marsh flooding
1 November 2006[a]	4.0 (Scolt Head Island)				13	Overtopping of gravel barrier at Cley and freshwater marsh flooding
17 March 2007[a]	3.35 (9)					Flooding at Brancaster Staithe, Wells and Blakeney. Coast road flooding
8 November 2007[a]	4.31 (1); 4.48 (2); 4.28 (3); 4.44 (4); 4.79 (5); 4.30 (6); 4.41 (7); 4.63 (8)			19		Described as a 'near miss' major storm surge
5 December 2013[a]	5.64 (1); 5.44 (2); 5.45 (3); 5.52 (4); 5.31 (5); 5.34 (6); 5.24 (7); 6.30 (8); 5.14 (9); 5.02 (10)	787		188		Major regional event. Flooding at Wells, Blakeney, Cley and Salthouse. Gravel barrier at Cley breached and freshwater marshes flooded. Freshwater marshes at Blakeney Freshes and Burnham Norton flooded. Arable land at Burnham Deepdale flooded.

[a]Storms highlighted in this paper.

[1]Note: Locations on the North Norfolk coast (see Figure 1): (1) Thornham; (2) Brancaster Staithe; (3) Burnham Deepdale; (4) Burnham Overy Staithe; (5) Wells Harbour Quay; (6) Stiffkey; (7) Morston; (8) Blakeney; (9) Cley; (10) Salthouse. Return Period (a1) = Immingham tide gauge (http:ww.surgewatch.org); Return Period (a2) = Cromer tide gauge (http:ww.surgewatch.org); Return Period (a3) = Lowestoft tide gauge (http:ww.surgewatch.org); Return Period (b1) = North Norfolk coast (East Anglian Coastal Group, 2010).

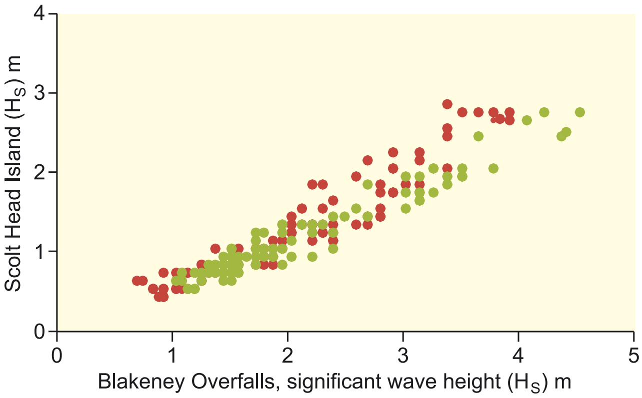

Figure 3. The relationship between significant wave height (H_s) at Blakeney Overafalls Wave rider buoy (for location see Figure 1B) and nearshore H_s from the AWAC buoys at Scolt Head Island ($y = 0.87x$; $r^2 = 0.85$) for the storms of March and November 2007. Wave data obtained from CeFAS wavenet data archive September 2006–October 2009 (http://www.cefas.defra.gov.uk/our-science/observing-and-modelling/monitoring-programmes/wavenet.aspx). This figure is available in colour online at wileyonlinelibrary.com/journal/espl

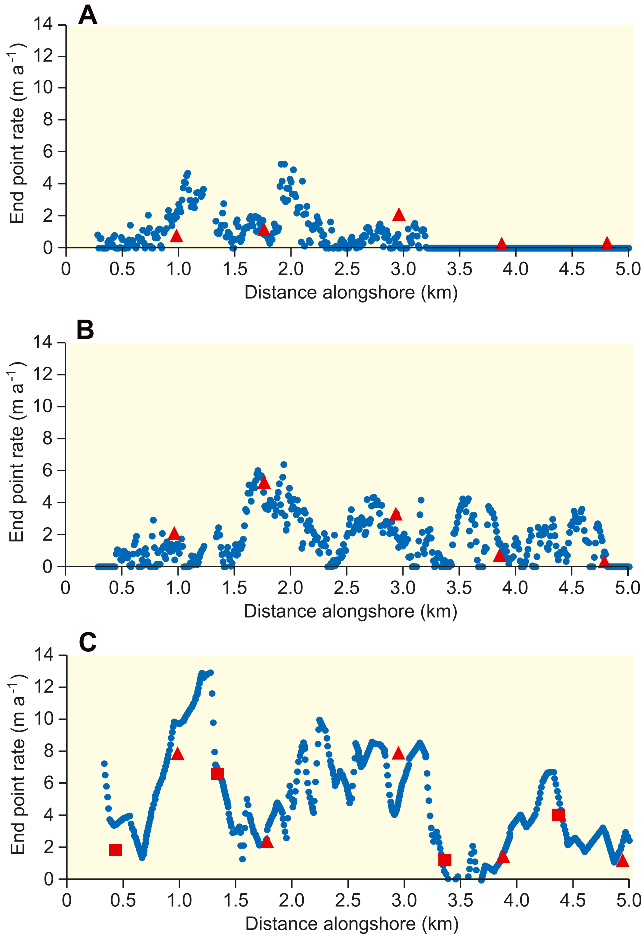

Figure 4. Alongshore DSAS analysis showing retreat at 10 m intervals along the barrier for years having more than 1 m inland retreat found in the cross-shore profiles. (A) DSAS end point rate (EPR) for summer 2006 to summer 2007, based upon digitized shorelines from Environment Agency aerial photography. This period included two storms in November 2006 and March 2007. (B) DSAS EPR for summer 2007 to summer 2008, based upon digitized shorelines from Environment Agency aerial photography. Retreat rate from Environment Agency cross-shore profile data are shown as squares. This period included one storm in November 2007. (C) DSAS EPR annual retreat for the period August 2013–August 2014 which included the 5–6 December 2013 storm surge. Squares and triangles show annual retreat derived from Environment Agency profile data. This figure is available in colour online at wileyonlinelibrary.com/journal/espl

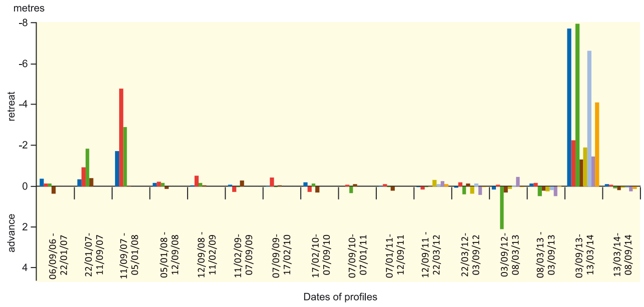

Figure 5. Shoreline retreat at Environment Agency cross-shore profile locations for the period 2006–2014 showing six-monthly retreat. This figure suggests clear phases of barrier stasis (or advance) interspersed with shoreline retreat especially evident in the periods September 2006–-September 2007, September 2007–December 2007 and September 2013–January 2014. This figure is available in colour online at wileyonlinelibrary.com/journal/espl

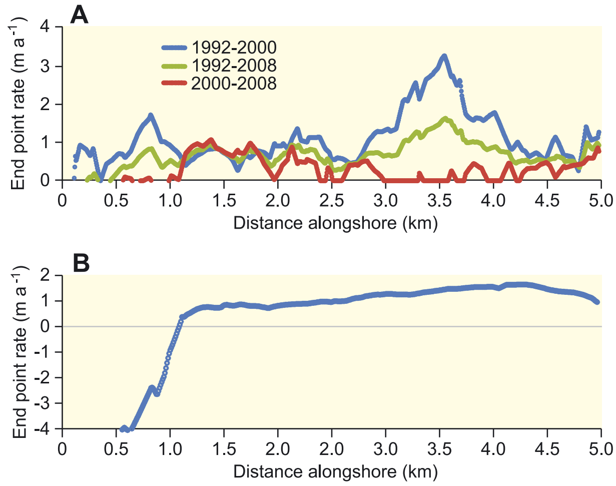

Figure 6. Alongshore DSAS end point rate (EPR) showing retreat at 10 m intervals along the barrier for (A) meso-term and (B) long-term timescales. This figure is available in colour online at wileyonlinelibrary.com/journal/espl

to 6.00 km, with the island mid-point shifting 0.60 km to the west since 1891.

Discussion

Shoreline change in a tidally-dominated barrier has occurred in clearly defined phases of activity and quiescence. The position of the dune crest has progressively been reset landwards since 2006 in three phases, with each shoreline translation averaging between 5 and 8 m. Such rates of migration under storm impacts on this coastline are by no means exceptional. In the major storm surge of 31 January to 1 February 1953 (Table II), Grove (1953) estimated 9–18 m of barrier retreat. For the 1978 surge event (Table II), Steers *et al.* (1979) reported even higher rates of landward migration, estimating an average of 20 m of retreat between Smuggler's Gap and Norton Hills (although this may have been be an over-estimation; see Spencer *et al.*, 2014). Of the four events identified, three appear to have crossed water level and wave setup thresholds for significant barrier movement. However, one storm (31 October–3 November 2006) generated no shoreline change. Thus the November 2006 event generated a large surge residual on a falling tide, while the March 2007 event was characterized by a small surge residual. Both events reached similar still water levels at Cromer. However, the March storm was followed by two days of high waves at Scolt Head Island, with the peak of wave activity being experienced on two successive high tides. The six monthly cross-shore profiles show a retreat rate of 0.13 ± 0.01 m for the November 2006 event and 0.48 ± 0.02 m for March 2007. Furthermore, the March storm was accompanied by a major morphological change on the island in the form of duneline breaching and the formation of an extensive washover fan towards the western end of the island (Michael Rooney, personal communication, 2007; Environment Agency, 2009). This resembles the creation of a 'breakthrough' in the centre of the island in 1953, when weather records from the Dowsing Light Vessel (53°35′N, 0°55′E) show that windspeeds in excess of 20 m s^{-1} (Beaufort Force 9, strong gale) were maintained for a 24 hour period over 31 January and 1 February 1953, generating significant wave heights of 7.8 m in 30 m water depths off the North Norfolk coast (Wolf and Flather, 2005). Thus echoing Sallenger (2000), a spectrum of no change – dune face erosion – major morphological change is possible, determined by both still water level and wave height at the shore, the magnitude and duration of these two components and the timing of their interaction (and see also Carter and Stone, 1989; Brooks *et al.*, 2012).

Over the meso-term, Figure 6A suggests strongly differentiated differences in retreat rates between large recession in the 1990s and much slower landward migration in the 2000s. This is the local expression of a regional landform response signal on the UK east coast, detected not only in the retreat rates of the soft rock Weybourne-Sheringham cliffs at the eastern margin of the study frontage, but also along clifflines of similar morphology on east-facing southern North Sea coasts at Covehithe, Suffolk and Walton-on-the-Naze, Essex (Brooks and Spencer, 2013). At Scolt Head Island, these differences cannot be explained by differences in storm surge event frequency; Table II shows that there were three such events in the period of high retreat compared to four events in the low retreat period. It is interesting to note, however, that the period of accelerated shore-normal change was accompanied by reduced alongshore change and vice versa; the western terminus of the island extended westwards by 35 m between 1992 and 2000 compared with 80 m between 2000 and 2008. It is unfortunate that the Blakeney Overfalls Wave rider Buoy only became operational in 2006 and that we therefore lack the detailed record of inter-decadal incident wave climate relatively close inshore that might inform this change in barrier dynamics.

The long-term, barrier-wide mean rate of shoreline retreat at Scolt Head Island over the period 1891–2013 was 1.15 m a^{-1}, equating to a landward translation of the barrier of 140 m. Our findings here demonstrate that between 5 and 8 m of barrier migration has typically accompanied recent high magnitude storms; this would suggest that this degree of shoreline change could be accomplished by between 17 to 28 storm impacts. Archival evidence for the occurrence of past storms, reported in Table II (for detailed sources see Supporting Information Table S1), shows 20 reported storm events since 1883. However, the preceding analysis of hydrodynamic forcing and morphological responses cautions against a simple correlation.

The short-term record of shoreline retreat of both high and low dune lines at Scolt Head Island shows a high degree of alongshore variability (Figure 4). This is carried through into the meso-term analysis (Figure 6A) although the locations of accelerated retreat do not necessarily coincide. However, at the centennial scale this alongshore variability is lost; the eroding sections of the barrier show a remarkably consistent rate of shoreline retreat, with a clear hinge point to the area of shoreline extension (Figure 6A). How can this time-dependent difference be explained? There is no evidence that this pattern results from the recovery of erosional hotspots by onshore sediment transport. At this timescale, Steers (1960) argued cogently that the high angle at which the laterals intersect the main barrier (Figure 1C) can be explained by the long-term landward translation of the barrier and, in the short-term, it is clear that there is little if any barrier recovery, by seaward extension, following storm impacts. Indeed, this pattern of change is strongly reminiscent of the same time-variant signal seen in systems that are only characterized by retreat, such as soft rock cliffs (e.g. Brooks and Spencer, 2010). An alternative explanation, following arguments that have been made for the evolution of the barrier shoreline of North Carolina (Lazarus and Murray, 2011; Lazarus *et al.*, 2011) is that localized storm impact signals become blurred at longer timescales by alongshore sediment transport. The exact details of such a mechanism, whilst plausible, are not well defined here. The traditional explanation for the progressive, if episodic, westward extension of Scolt Head Island is longshore transport from the east from a 'drift parting' near Sheringham, the estimated transport rate being dependent upon the particle size distribution, varying between 190 and 60 m^3 a^{-1} (HR Wallingford, 2002). Seabed sediments and facies mapping suggests that the transport direction is the reverse offshore, at least below the 7 m contour. This suggests that sand and shingle is being transported to the west on the beach face, but that sand is transported to the east if it is carried offshore from the steep beach face onto the extensive subtidal Burnham Flats, perhaps under storm surge conditions (East Anglian Coastal Group, 2010). Furthermore, an alternative model argues that sediment transport on the beach face is from west to east, with by-passing of the Brancaster Staithe Harbour Channel by episodic sand-waves moving through the ebb tidal delta. These easterly-moving sand waves then weld onto the western extremities of the barrier, explaining its westward growth. Using barrier lengthening and tidal inlet narrowing in the Wadden Sea as an analogy, where long-term decreases in backbarrier areas have followed several phases of historical land claim (Fitzgerald *et al.*, 1984), post-nineteenth century extension of the Scolt barrier may also have followed the enclosure of > 200 ha of saltmarsh behind an earthen embankment east of Burnham Deepdale in 1882 (Figure 1B). This would have reduced the tidal flow through the Harbour Channel to allow more rapid easterly passage of sandwaves across it (Royal Haskoning and Pethick, 2003).

Finally, Horsburgh and Lowe (2013) have argued that whilst there is no significant evidence for future changes in storm-related extreme sea levels for the UK, it is not unreasonable to assume that future changes in extreme sea level will be governed by mean sea-level rise. Woodworth *et al.* (2009) demonstrate that absolute mean sea level (AMSL) rose by 1.4 ± 0.2 mm a^{-1} around the UK over the twentieth century, suggesting that the baseline water level rose by 16 ± 0.3 cm between 1891 and 2010. However, for more recent periods, Wahl *et al.* (2013) found a relative sea level rise of 2.7 ± 0.4 mm a^{-1} (1900–2011), 3.6 ± 0.5 mm a^{-1} (1980–2011) and 4.4 ±1.1 mm a^{-1} (1993–2011) in the Lowestoft tide gauge. If there is a broad correlation between rates of barrier retreat and sea level rise then this would suggest that a considerable acceleration in the rate of barrier migration might be expected over the remainder of the twenty-first century.

Conclusions

The analysis developed in this paper provides valuable insights into the importance of storm impacts on barrier and shoreline dynamics and shows how the richness and detail in contemporary data can be used to examine the thresholds for barrier retreat. We have mined and synchronized a range of data sets on shoreline movement and hydrodynamics to reconstruct storm impacts on a retreating barrier. We have demonstrated how shoreline change in the recent past (last decade) is most likely to have been driven by individual storms that cross water level and especially wave energy thresholds. The better identification of these thresholds offers the possibility of better explanations of the characteristic pattern of periods of enhanced retreat being interspersed with periods of low, or no retreat. However, explaining meso-term and long-term patterns in barrier dynamics remains challenging, particularly in the absence of corresponding forcing data.

Acknowledgements—This paper was completed while the first author (SB) was a recipient of a Leverhulme Research Fellowship (RF-2015-045) for a project entitled 'Development and application of a shoreline response model'. This paper is a contribution to NERC BESS Consortium grant 'A hierarchical approach to the examination of the relationship between biodiversity and ecosystem service flows across coastal margins' (grant reference NE/J015423/1). Table I reports information gathered as part of an EU FP7 Collaborative Project (grant agreement no: 603458) 'Resilience-increasing Strategies for Coasts – toolkit' (http://www.risckit.eu). The authors thank Ben Evans and James Tempest for considerable assistance with field data collection, often under challenging field conditions. David Welsh of the UK Environment Agency kindly assisted with the supply of aerial photographs and profile data.

References

Andrews JE, Boomer I, Bailiff I, Balson P, Bristow C, Chroston PN, Funnell BM, Harwood GM, Jones RW, Maher BA, Shimmield G. 2000. Sedimentary evolution of the north Norfolk barrier coastline in the context of Holocene sea-level change. In *Holocene Land–Ocean Interaction and Environmental Change around the North Sea*, Shennan I, Andrews J (eds), Special Publication 166. Geological Society: London; 219–251. DOI. 10.1144/GSL.SP.2000.166.01.12

Brooks SM, Spencer T. 2010. Temporal and spatial variations in recession rates and sediment release from soft rock cliffs, Suffolk coast, UK. *Geomorphology* **124**: 26–41. DOI:10.1016/j.geomorph.2010.08.005.

Brooks SM, Spencer T. 2013. Importance of decadal scale variability in shoreline response: examples from soft rock cliffs, East Anglian coast, UK. *Journal of Coastal Conservation* **18**: 581–593. DOI. 10.1007/s11852-013-0279-7

Brooks SM, Spencer T, Boreham S. 2012. Deriving mechanisms and thresholds for cliff retreat in soft-rock cliffs under changing climates: rapidly retreating cliffs of the Suffolk coast, UK. *Geomorphology* **153–154**: 48–60. DOI:10.1016/j.geomorph.2012.02.007.

Carter RWG, Stone GW. 1989. Mechanisms associated with the erosion of sand dune cliffs, Magilligan, Northern Ireland. *Earth Surface Processes and Landforms* **14**: 1–10. DOI:10.1002/esp.3290140102.

Church JA, Clark PU, Cazenave A. 2013. Sea level change. In *Climate Change 2013: The Physical Science Basis*, Stocker TF et al. (eds). Contribution of Working Group I to the Fifth Assessment Report of the Intergovernmental Panel on Climate Change. Cambridge University Press: Cambridge.

Cowell PJ, Roy PS, Jones RA. 1995. Simulation of large-scale coasts change using a morphological-behaviour model. *Marine Geology* **126**: 45–61. DOI:10.1016/0025-3227(95)00065-7.

Donnelly C, Kraus N, Larson M. 2006. State of knowledge on measurement and modeling of coastal overwash. *Journal of Coastal Research* **22**: 965–991. DOI:10.2112/04-0431.1.

East Anglian Coastal Group. 2010. *North Norfolk Shoreline Management Plan Final Plan 2010.* http://www.eacg.org.uk/docs/smp5/the%20smp%20main%20report.pdf

Environment Agency. 2009. *Sea State Report Norfolk (Year 1 Oct 2006–Sept 2007) (RP011/N/2009). Shoreline Monitoring Group*. Environment Agency: Peterborough.

Environment Agency. 2014. *Sea State Report Norfolk Year 3 and Summary for October 2006–September 2009 (RP039/N/2014). Shoreline Monitoring Group*. Environment Agency: Peterborough.

Fitzgerald DM, Penland S, Nummedal D. 1984. Control of barrier island shape by inlet sediment bypassing: East Frisian Islands, West Germany. *Marine Geology* **60**: 355–376.

Fitzgerald DM, Fenster MS, Argow BA, Buynevich IV. 2008. Coastal impacts due to sea-level rise. *Annual Review of Earth and Planetary Sciences* **36**: 601–647. DOI:10.1146/annurev.earth.35.031306.140139.

French JR. 1993. Numerical modelling of vertical marsh growth and response to rising sea-level, Norfolk, UK. *Earth Surface Processes and Landforms* **18**: 63–81. DOI. 10.1002/esp.3290180105

Gerritsen H. 2005. What happened in 1953? The Big Flood in the Netherlands in retrospect. *Philosophical Transactions of the Royal Society of London* **363A**: 1271–1291. DOI:10.1098/rsta.2005.1568.

Grove AT. 1953. IV. The sea flood on the coasts of Norfolk and Suffolk. *Geography* **38**: 164–170.

Haigh ID, Wadey MP, Gallop SL, Loehr H, Nicholls RJ, Horsburgh K, Brown JM, Bradshaw E. 2015. A user-friendly database of coastal flooding in the United Kingdom from 1915–2014. *Nature Scientific Data* **2**: 150021. 1–13. DOI. 10.1038/sdata.2015.21

Hayes MO. 1979. Barrier island morphology as a function of tidal and wave regime. In *Barrier Islands: From the Gulf of St. Lawrence to the Gulf of Mexico*, Leatherman SP (ed). Academic Press: New York; 1–28.

Horsburgh K, Lowe J. 2013. Impacts of climate change in sea level. *Marine Climate Change Impacts Partnership: Science Review*: 27–33. DOI:10.14465/2013.arc04.027-033.

Wallingford HR. 2002. *Southern North Sea Sediment Transport Study – Phase 2*. Sediment Transport Report. Prepared for Great Yarmouth Borough Council by HR Wallingford in association with CEFAS/UEA, Posford Haskoning and Dr B D'Olier. Report EX4526. HR Wallingford: Wallingford.

Intergovernmental Panel on Climate Change (IPCC). 2013. Summary for policymakers. In *Climate Change 2013: The Physical Science Basis*, Stocker TF *et al.* (eds), Contribution of Working Group I to the Fifth Assessment Report of the Intergovernmental Panel on Climate Change. Cambridge University Press: Cambridge.

Jiménez JA, Sánchez-Arcilla A. 2004. A long-term (decadal scale) evolution model for microtidal barrier systems. *Coastal Engineering* **51**: 749–764. DOI:10.1016/j.coastaleng.2004.07.007.

Lamb H, Frydendahl K. 1991. *Historic Storms of the North Sea, British Isles and Northwest Europe*. Cambridge University Press: Cambridge.

Lazarus ED, Murray AB. 2011. An integrated hypothesis for regional patterns of shoreline change along the northern North Carolina Outer Banks, USA. *Marine Geology* **281**: 85–90. DOI:10.1016/j.margeo.2011.02.002.

Lazarus E, Ashton A, Murray AB, Tebbens S, Burroughs S. 2011. Cumulative versus transient shoreline change: dependencies on temporal and spatial scale. *Journal of Geophysical Research* **116**: F02014. DOI:10.1029/2010JF001835.

Lazarus ED, Ashton AD, Murray AB. 2012. Large scale patterns in hurricane driven shoreline change. In *Extreme Events and Natural Hazards: The Complexity Perspective*, Surjalal Sharma A, Bunde E, Dimri VP, Baker DN (eds). Geophysical Monographs 196. American Geophysical Union/Wiley: Chichester; 127–138. DOI. 10.1029/2011GM001074

Lee EM. 2008. Coastal cliff behaviour: observations on the relationship between beach levels and recession rates. *Geomorphology* **101**: 558–571. DOI:10.1016/j.geomorph.2008.02.010.

Long JW, de Bakker ATM, Plant NG. 2014. Scaling coastal dune elevation changes across storm-impact regimes. *Geophysical Research Letters* **41**: 2899–2906. DOI:10.1002/2014GL059616.

Lorenzo-Trueba J, Ashton AD. 2014. Rollover, drowning, and discontinuous retreat: distinct modes of barrier response to sea-level rise arising from a simple morphodynamic model. *Journal of Geophysical Research: Earth Surface* **119**: 779–801. DOI:10.1002/2013JF002941.

McBride RA, Anderson JB, Buynevich IV, Cleary W, Fenster MS, Fitzgerald DM, Harris MS, Hein CJ, Klein AHF, Liu B, de Menezes JT, Pejrup M, Riggs SR, Short AD, Stone GW, Wallace DJ, Wang P. 2013. Morphodynamics of barrier systems: a synthesis. In *Treatise on Geomorphology, Coastal and Submarine Geomorphology,* Shroder J, Sherman DJ (eds). Academic Press: San Diego, CA; 166–244.

Masetti RS, Fagherazzi S, Montanari A. 2008. Application of a barrier island translation model to the millennial-scale evolution of Sand Key, Florida. *Continental Shelf Research* **28**: 1116–1126. DOI:10.1016/j.csr.2008.02.021.

Mellett CL, Hodgson DM, Lang A, Mauz B, Selby I, Plater AJ. 2012. Preservation of a drowned gravel barrier complex: A landscape evolution study from the north-eastern English Channel. *Marine Geology* **315–318**: 115–131. DOI:10.1016/j.margeo.2012.04.008.

Moore LJ, List JH, Williams SJ, Stolper D. 2010. Complexities in barrier island response to sea level rise: insights from numerical model experiments, North Carolina Outer Banks. *Journal of Geophysical Research* **115**: F03004. DOI:10.1029/2009JF001299.

Otvos EG. 2012. Coastal barriers – nomenclature, processes and classification issues. *Geomorphology* **139-140**: 39–52. DOI:10.1016/j.geomorph.2011.10.037.

Plant NG, Stockdon HF. 2012. Probabilistic prediction of barrier-island response to hurricanes. *Journal of Geophysical Research* **117**: F03015. DOI:10.1029/2011JF002326.

Pugh D, Woodworth P. 2014. *Sea-level Science: Understanding Tides, Surges, Tsunamis and Mean Sea-level Changes*. Cambridge University Press: Cambridge.

Royal Haskoning, Pethick J. 2003. *North Norfolk Coast Coastal Habitat Management Plan Final Report January 2003*. Royal Haskoning: Peterborough.

Sallenger AH, Jr 2000. Storm impact scale for barrier islands. *Journal of Coastal Research* **16**: 890–895. DOI:10.2307/4300099.

Sanders JE, Kumar N. 1975. Evidence of shoreface retreat and in-place "drowning" during Holocene submergence of barriers, shelf off Fire Island, New York. *Geological Society of America Bulletin* **86**: 65–76. DOI:10.1130/0016-7606(1975)86<65:EOSRAI>2.0.CO;2.

Sherwood CR, Long JW, Dickhudt PJ, Dalyander PS, Thompson DM, Plant NG. 2014. Inundation of a barrier island (Chandeleur Islands, Louisiana, USA) during a hurricane: observed water-level gradients and modeled seaward sand transport. *Journal of Geophysical Research Earth Surface* **119**: 1498–1515. DOI:10.1002/2013JF003069.

Spencer T, Brooks SM, Möller I, Evans BR. 2014. Where local matters: impacts of a major North Sea storm surge. *EOS, Transactions of the American Geophysical Union* **95**: 269–270. DOI:10.1002/2014EO300002.

Steers JA. 1960. *Scolt Head Island*. Heffers: Cambridge.

Steers JA, Bayliss-Smith TP, Stoddart DR, Spencer T, Durbridge PM. 1979. The storm surge of 11 January 1978 on the east coast of England. *Geographical Journal* **145**: 192–205. DOI:10.2307/634386.

Stockdon HF, Sallenger AH, Jr, Holman RA, Howd PA. 2007. A simple model for the spatially-variable coastal response to hurricanes. *Marine Geology* **238**: 1–20. DOI:10.1016/j.margeo.2006.11.004.

Thieler ER, Himmelstoss EA, Zichichi JL, Ergul A. 2009. *Digital Shoreline Analysis System (DSAS) Version 4.0 – An ArcGIS Extension for Calculating Shoreline Change*, US Geological Survey Open-File Report 2008-1278.US Geological Survey: Reston, VA.

Wahl T, Haigh ID, Woodworth PL, Albrecht F, Dillingh D, Jensen J, Nicholls R, Weisse R, Wöppelmann G. 2013. Observed mean sea level changes around the North Sea coastline from 1800 to the present. *Earth-Science Reviews* **124**: 51–67. DOI:10.1016/j.earscirev.2013.05.003.

Weisse R, Bellafiore D, Menéndez M, Méndez F, Nicholls RJ, Umgiesser G, Willems P. 2014. Changing extreme sea levels along European coasts. *Coastal Engineering* **87**: 4–14. DOI:10.1016/j.coastaleng.2013.10.017.

Wolf J, Flather RA. 2005. Modelling waves and surges during the 1953 storm. *Philosophical Transactions of the Royal Society of London* **363A**: 1359–1375. DOI. 10.1098/rsta.2005.1572

Woodworth PL, Teferle FN, Bingley RM, Shennan I, Williams SDP. 2009. Trends in UK mean sea level revisited. *Geophysical Journal International* **176**: 19–30. DOI. 10.1111/j.1365-246X.2008

Zhang K, Leatherman S. 2011. Barrier island population along the U.S. Atlantic and Gulf Coasts. *Journal of Coastal Research* **27**: 356–363. DOI:10.2112/JCOASTRES-D-10-00126.1.

SUPPORTING INFORMATION

Additional supporting information may be found in the online version of this article at the publisher's web site.

